Electron hole formation in acidic zeolite catalysts

Xavier Solans-Monfort, Vicenç Branchadell, and Mariona Sodupe
Departament de Química, Universitat Autònoma de Barcelona Bellaterra 08193, Spain

Marek Sierka and Joachim Sauer[a)]
Institut für Chemie, Humboldt-Universität zu Berlin Berlin D-10099, Germany

(Received 11 May 2004; accepted 17 June 2004)

The formation of an electron hole on an AlO_4H center of the H-ZSM-5 zeolite has been studied by a hybrid quantum mechanics/shell-model ion-pair potential approach. The Becke-3-Lee-Yang-Parr (B3LYP) and Becke-Half&Half-Lee-Yang-Parr (BHLYP) hybrid density functionals yield electron holes of different nature, a delocalized hole for B3LYP and a hole localized on one oxygen atom for BHLYP. Comparison with coupled cluster calculations including single and double substitutions and with perturbative treatment of triple substitutions CCSD(T) and with experimental data for similar systems indicate that the localized description obtained with BHLYP is more accurate. Generation of the electron hole produces a substantial geometry relaxation, in particular an elongation of the Al-O distance to the oxygen atom with the unpaired electron. The zeolite framework stabilizes the positive charge by long-range effects. Our best estimates for the vertical and adiabatic ionization energies are 9.6–10.1 and 8.4–8.9 eV, respectively. Calculations for silicalite, the all-silica form of ZSM-5, also yield a localized electron hole, but the energy cost of the process is larger by 0.6–0.7 eV. The deprotonation energy of H-ZSM-5 is found to decrease from 12.86 to 11.40 eV upon electron hole formation. © *2004 American Institute of Physics.* [DOI: 10.1063/1.1781122]

I. INTRODUCTION

Proton exchanged zeolites are important acidic industrial catalysts.[1,2] One of the most interesting properties of acid zeolites is their ability to spontaneously generate organic radical cations upon adsorption of electron donor molecules.[3–5] These species can also be generated by γ radiation of zeolites containing organic molecules.[3,6,7] The γ radiation generates a free electron and a hole in the zeolite in such a way that an electron transfer from the guest to the zeolite can occur leading to the desired radical cation. This process is suggested to occur when the ionization energy of the guest molecule is lower than 10.0–10.5 eV.[7]

Radical cations are stabilized by the zeolite and protected from reagents.[4] Consequently, the observed lifetimes of radical cations in zeolites are longer than in solution. Because of that, the study of these species has attracted considerable attention in the last years. Furthermore, some radical cation species have been suggested as intermediates in several catalytic processes.[1] The generation of organic radical cations in zeolites and their reactions have recently been reviewed.[8] However, the formation of radical cation sites (electron holes) in zeolites is not well understood.

A first step to understand how these species are generated is to analyze the properties of the zeolite upon formation of an electron vacancy. The comprehension of the electron hole nature can provide important insights on the effects of oxidation on the Brønsted acid site as well as on the reactivity of adsorbed molecules in irradiated zeolites.

Similar electron vacancies have been described in related materials.[9–14] In particular, several authors have considered the neutral substitution impurity in α-quartz, $[AlO_4]^0$, both from an experimental and a theoretical point of view. Using electron paramagnetic resonance (EPR) spectroscopy the experimental studies have shown that the electron hole trapped in the neutral defect center $[AlO_4]^0$ is localized on one of the oxygen atoms, which is accompanied by a substantial lattice distortion.[14] The most important change is the elongation of the Al-O bond of the hole. It has been shown that pure gradient corrected density functionals or the hybrid Becke-3-Lee-Yang-Parr hybrid functional (B3LYP) are not accurate enough to describe the $[AlO_4]^0$ defect, since they yield a hole delocalized over all oxygen atoms bonded to aluminum. On the contrary, the Hartree-Fock method (HF) or the HF-Lee-Yang-Parr functional (HF-LYP) which uses 100% of exact exchange provide a localized hole. This is corroborated by the agreement between experimental EPR hyperfine coupling parameters with those computed by HF and HF-LYP.[13] This observation can be explained taking into account that pure density functional methods have been shown to overstabilize delocalized radical cations with long bond distances, due to a bad cancellation of the self-interaction by the exchange functional. Since exact exchange rigorously corrects for self-interaction, its inclusion in the functional partially corrects for this overstabilization.[15] However, it is difficult to know *a priori* how much exact exchange has to be included in the functional to get a proper description of the system.

In this study electron hole formation in the H-ZSM-5 zeolite is examined from a computational point of view. Our main goals are to determine the structural changes induced by the electron hole as well as its influence on the acidity of

a)Author to whom correspondence should be addressed. Electronic mail: sek.qc@chemie.hu-berlin.de

the Brønsted site. Moreover, the ionization energy of H-ZSM-5 has been computed and compared to that of SiO_2, which is known from experiments to lie between 10.2 and 10.6 eV.[16] For aluminum-poor zeolites (Si/Al=13) valence band spectra have been found to be similar to that of SiO_2, the electron binding energy being slightly lower.[17] Calculations have been done using the hybrid quantum mechanics/analytical potential function (QM-pot) embedded cluster approach.[18,19] This scheme has been successfully used to understand the structure, bonding properties, and reactivity of the active sites of many zeolites.[18,20–22]

II. COMPUTATIONAL DETAILS

The QM-Pot methodology divides the whole system (S) in two parts: the inner part, which is treated with quantum mechanical (QM) methods and includes the major part of the chemical problem, and the outer part which is treated by a parametrized interatomic potential (Pot) with periodic boundary conditions. Chemical bonds between inner and outer parts are saturated with link hydrogen atoms. The link atoms and the inner part form the cluster (C). The QM-Pot energy of the whole system is obtained by a subtraction scheme of three independent calculations,

$$E_{\text{QM-POT}}(S)=E_{\text{QM}}(C)+E_{\text{Pot}}(S)-E_{\text{Pot}}(C), \tag{1}$$

where $E_{\text{QM}}(C)$ represents the energy of the cluster obtained with quantum mechanics, and $E_{\text{Pot}}(S)$ and $E_{\text{Pot}}(C)$ are the energies calculated with the interatomic potential of the whole system and cluster, respectively. Calculations have been performed using the QMPOT program,[18] which uses the TURBOMOLE package[23] for the QM part and GULP (Ref. 24) for the interatomic potential.

The formation of an electron hole has been studied in two different forms of the ZSM-5 zeolite: H-ZSM-5 which has an $Al(O\text{-})_4H$ site in a nanoporous SiO_2 framework and silicalite which is a pure silica form with the same pore structure. ZSM-5 occurs in two crystal structures, as an orthorhombic or as a monoclinic lattice depending on the temperature.[25] Our studies use the orthorhombic form with cell parameters obtained from constant pressure calculations using the shell-model ion-pair potential alone. The H-ZSM-5 model has one aluminum atom per unit cell (Si/Al=95) with the Al atom located at the T7 crystallographic position. This is the most favourable substitution site found in computational studies.[22,26] It was also adopted before in a proton mobility study.[21]

Figure 1 shows the different clusters considered for the inner part. 5T embedded cluster is the standard model used for structure determination, analysis of the process, and energy evaluation. Thus, full optimizations of the embedded 5T cluster have been made with full relaxation of the embedding periodic lattice (constant pressure). An extended 25T cluster model is used for checking the convergence of the QM-Pot scheme with increasing cluster size.

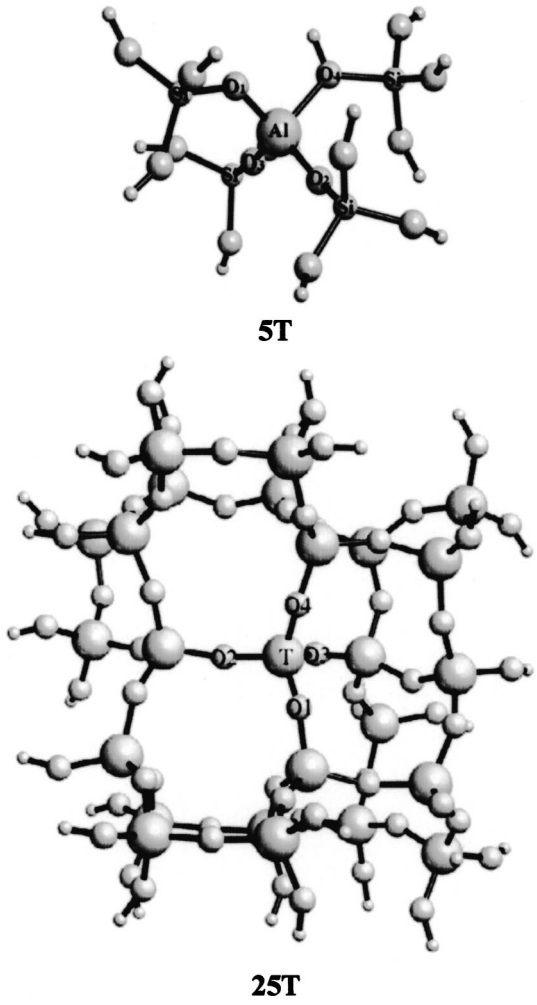

FIG. 1. Inner part (embedded cluster) employed in QM-Pot calculations.

It is constructed from the 5T optimized geometries and single point calculations have been performed only.

For the QM part, we have used density functional theory (DFT) with the hybrid B3LYP (Refs. 27 and 28) and BHLYP (Refs. 28 and 29) functionals and the $6\text{-}31++G(d,p)$ basis set.[30] As mentioned in the Introduction, pure density functional methods overstabilize delocalized radical cations.[15] Because of that, we have also applied the accurate CCSD(T) method (Ref. 31) to the 1T cluster models, $Al(OH)_4H$ and $Si(OH)_4$. In these models the link hydrogen atoms have been set at O-H bond distances of 0.9628 and 0.9666 Å when the central atom is aluminum and silicon, respectively. CCSD(T) open shell calculations have been made using a spin restricted formalism[32] as implemented in MOLPRO (Refs. 33 and 34) to avoid spin contamination. Dunning's correlation consistent polarized basis sets up to quadrupole zeta cc-pVQZ (Ref. 35) and the augmented basis sets up to triple-zeta (aug-cc-pVTZ, Ref. 36), have been used to extrapolate to complete basis set limit.[37]

The interatomic potential for the periodic outer part is a shell-model ion-pair potential[38] with parameters optimized by Sierka and Sauer on DFT results for the neutral system.[39] This potential takes the polarizability of the oxygen ions into account and, hence, is able to describe the polarization of the

zeolite framework by the positive charge created on electron hole formation. For the ionized system two different parametrizations of the electron hole have been considered. In both cases, only the shell charge has been modified. The first parametrization removes one third of electron from the three oxygen atoms around aluminum which do not support the proton (L1/3), while the second parametrization removes a whole electron from only one of the oxygen atoms (L1). Similar approaches which modify only shell parameters can be found in the literature.[9,40] Assuming that the low level does not produce important geometry changes, the differences between L1/3 and L1 parametrizations will give us an idea of how the electron hole is stabilized by long range effects and how much this effect depends on details of the embedding potential.

Applying periodic boundary conditions to the calculation of $E_{\mathrm{Pot}}(S)$ for the ionized system involves a positive charge in every unit cell which does not represent a realistic system. To avoid diverging lattice sums we have included a neutralizing background charge for the ionized unit cells. However, even in the presence of a neutralizing background the interaction between charged defects in different cells is still present. Extrapolation to the situation of an isolated defect is possible by subtracting the aperiodic correction (APC),[41]

$$\mathrm{APC} = E(+)/\varepsilon_z, \tag{2}$$

where $E(+)$ is computed classically as the energy of a periodic array of positive charges with a neutralizing background in a dielectric. The dielectric constant ε_z is equal to that of the perfect zeolite and calculated as one-third of the trace of the static dielectric tensor. For the unit cells adopted in this study the correction is 0.34 eV. To test the accuracy of this correction we have constructed a supercell by doubling the unit cell size of H-ZSM-5. After applying the aperiodic correction, the ionization energies obtained for the single cell and the double cell differ by 0.03 eV only, which indicates the reliability of the aperiodic correction. Note that this type of correction is not a specific feature of QM-Pot, it would also be necessary if we were able to do a fully periodic quantum mechanical calculation.

The ionization energy obtained by the QM-Pot method can be decomposed into the direct quantum mechanical contribution, QM, a long-range correction, LR, and the aperiodic correction, APC.

TABLE I. T-O distances (in Å) for neutral, deprotonated, and ionized systems using embedded 5T clusters. The proton is attached to O_4.

		T-O_1	T-O_2	T-O_3	T-O_4
H-ZSM-5 (B3LYP)	Neutral	1.731	1.723	1.704	1.929
	Ionized:L1/3	1.742	1.717	1.711	1.883
	Ionized:L1	1.763	1.689	1.752	1.872
H-ZSM-5 (BHLYP)	Neutral	1.717	1.710	1.693	1.915
	Ionized:L1/3	1.684	1.895	1.655	1.861
	Ionized:L1	1.688	1.871	1.663	1.855
H-ZSM-5 (BHLYP)	Deprotonated	1.738	1.731	1.746	1.739
	Deprotonated, Ionized:L1	1.704	1.910	1.706	1.698
Silicalite (BHLYP)	Neutral	1.615	1.609	1.619	1.620
	Ionized:L1	1.778	1.580	1.582	1.586

$$I(\mathrm{QM\text{-}Pot}) = I(\mathrm{QM}) + I(\mathrm{LR}) + \mathrm{APC} \tag{3}$$

with

$$I(\mathrm{QM}) = E_{\mathrm{QM}}(C^{\mathrm{Ionized}}) - E_{\mathrm{QM}}(C^{\mathrm{Neutral}}) \tag{4}$$

and

$$I(\mathrm{LR}) = [E_{\mathrm{Pot}}(S^{\mathrm{Ionized}}) - E_{\mathrm{Pot}}(C^{\mathrm{Ionized}})] - [E_{\mathrm{Pot}}(S^{\mathrm{Neutral}}) - E_{\mathrm{Pot}}(C^{\mathrm{Neutral}})]. \tag{5}$$

Note that $I(\mathrm{QM})$ is not identical with the QM result for a nonembedded cluster because the structure has been optimized at the QM-Pot level.

III. RESULTS

A. Electron hole in H-ZSM-5

Table I presents the T-O distances, while Table II shows the spin distribution based on occupation numbers[42] over the four oxygen atoms bonded to the central tetrahedron. For the neutral system, the three Al-O distances corresponding to the nonprotonated oxygen atoms are very similar, the computed values ranging from 1.704 Å to 1.731 Å with B3LYP and from 1.693 Å to 1.717 Å with BHLYP. The Al-O_4 distance is considerably larger (1.929 Å and 1.915 Å, respectively) due to the protonation of oxygen. The creation of an electron vacancy produces significant changes. In all cases the Al-O_4(H) distance slightly decreases. However, the changes

TABLE II. Spin populations based on occupation numbers (Ref. 40) for electron holes in neutral and deprotonated zeolites using embedded 5T clusters (Mulliken analysis in parenthesis).

		Spin population[a]			
		O_1	O_2	O_3	O_4
H-ZSM-5	B3LYP:L1/3	0.23(0.24)	0.19(0.18)	0.19(0.18)	0.00(0.00)
	B3LYP:L1	0.27(0.27)	0.07(0.06)	0.27(0.26)	0.00(0.00)
H-ZSM-5	BHLYP:L1/3	0.02(0.03)	0.98(0.92)	0.01(0.01)	0.00(0.00)
	BHLYP:L1	0.05(0.05)	1.00(0.93)	0.01(0.01)	0.00(0.00)
H-ZSM-5 deprotonated	BHLYP:L1	0.03(0.03)	0.99(0.93)	0.00(0.00)	0.01(0.00)
Silicalite	BHLYP:L1	0.96(0.91)	0.04(0.06)	0.04(0.03)	0.01(0.00)

TABLE III. Vertical I_V and adiabatic ionization energies I_A (in eV) for H-ZSM-5 (5T cluster) calculated with different density functionals and parametrizations for the embedding potential.

High level	Pot	I_V	QM[a]	LR[b]+APC[c]	I_A	QM[a]	LR[b]+APC[c]
B3LYP	L1/3	7.88	8.79	−0.91	7.48	8.68	−1.20
	L1	7.83	8.79	−0.96	7.22	8.59	−1.36
BHLYP	L1/3	9.00	9.93	−0.97	7.85	8.87	−1.02
	L1	8.94	9.93	−0.99	7.74	9.26	−1.52

[a]QM contribution, defined by Eq. (4).
[b]Long-range contribution, defined by Eq. (5).
[c]Aperiodic correction, defined by Eq. (12).

on the other Al-O distances depend on the amount of exact exchange included in the functional (B3LYP or BHLYP) and on the details of the low level model of the solid. At the B3LYP level, the largest variations are observed for the L1 model, for which the Al-O_2 distance becomes 0.03 Å shorter whereas the other two Al-O distances increase by approximately the same amount.

At the BHLYP level, one of the three Al-O distances related with nonprotonated oxygen atoms presents an elongation of at least 0.16 Å, while the other two Al-O distances slightly decrease (by 0.03–0.04 Å). Moreover, there is also a significant geometry change related to the coordination geometry around the central aluminum. In the neutral system this coordination environment is tetrahedral as expected. However, in all three ionized BHLYP structures the geometry evolves to a trigonal pyramid structure where the ligand at the apical position corresponds to the nonprotonated oxygen with the longest Al-O_2 distance. The effects of the hole parametrization in the embedding shell-model potential (L1/3 versus L1 model in the low-level calculation) on the geometry parameters are less significant than those at the B3LYP level. However, the tendency to slightly reduce the longest Al-O_2 distance is still observed when the full charge is on one oxygen in the low-level description part (L1 model).

The differences between the geometrical parameters obtained with the B3LYP and BHLYP functional arise from the different spin distribution (Table II). B3LYP delocalizes the spin density over the three nonprotonated oxygen atoms whereas with BHLYP the spin density is mainly localized at O_2, the nonprotonated oxygen with the longest Al-O distance. Thus, the elongation of the Al-O bond leads to a radical system with the proton and the spin density located at different oxygen sites. Table II also indicates that the major part of the spin is on the oxygen atoms bonded to central aluminum, indicating that a 5T cluster for the high level (DFT) part is large enough to yield a qualitatively correct electronic structure. It is also important that the correct localization of the electron hole at one oxygen site is obtained, irrespective of whether the L1/3 or L1 parametrization of the embedding potential is used, provided that BHLYP is applied.

As detailed in the Introduction, previous studies on $[AlO_4]^0$ defects on α-quartz[13] showed similar trends as we find here for H-ZSM-5. These studies have concluded that BLYP and B3LYP do not properly describe the nature of the $[AlO_4]^0$ defect, while unrestricted Hartree-Fock (UHF) or UHF-LYP do. The present work on ionized H-ZSM-5 shows that inclusion of 50% of exact exchange is sufficient to get a qualitatively correct description of the electron hole.

The ionization energy of H-ZSM-5, I, computed with B3LYP and BHLYP and for the two different embedding potentials is shown in Table III. The total ionization energy is decomposed in two terms: the QM contribution, which corresponds to the ionization energy of the cluster computed at the QM level and the long-range term (LR), which accounts for the effect of including the whole framework at the low level (embedding shell model ion-pair potential). Note that the latter is given together with the aperiodic correction, APC. The vertical ionization energies obtained with BHLYP are always about 1.1 eV higher than those obtained with B3LYP. When the ionized system is allowed to relax, the ionization energy decreases considerably indicating that the geometry relaxation is very important, especially with BHLYP (around 1.2 eV) due to the large geometry distortion. Thus, the differences between B3LYP and BHLYP are much smaller for the adiabatic ionization energies I_A (0.4–0.5 eV) than for the vertical ones (1.1 eV). Again, the L1/3 and L1 parametrizations of the embedding potential change the BHLYP total ionization energies by 0.06 (vertical) and 0.11 eV (adiabatic) only, indicating stability of the results. However, the L1 parametrization which assumes a localized hole is the more realistic one and will be further used in this study.

As mentioned, B3LYP and BHLYP functionals provide different pictures of the electron hole in ionized H-ZSM-5. As a further test which density functional describes better the ionization energy of H-ZSM-5, we have made single point calculations with the CCSD(T)/6-31++G(d,p) method for the 1T cluster at the structure obtained by the 5T embedded cluster calculations. The results are presented in Table IV.

TABLE IV. DFT-6-31++G(d,p) and CCSD(T)/6-31++G(d,p) single point ionization energies (in eV) for the 1T cluster model at the geometries optimized for the 5T embedded clusters by B3LYP and BHLYP.

	Geometry	B3LYP	CCSD(T)
H-ZSM-5	B3LYP:L1/3	9.10	9.97
	B3LYP:L1	9.16	9.82
	Geometry	BHLYP	CCSD(T)
H-ZSM-5	BHLYP:L1/3	9.43	9.51
	BHLYP:L1	9.47	9.60
Silicalite	BHLYP:L1	10.32	10.60

CCSD(T) values are always significantly larger than the B3LYP ones, the average deviation being 0.77 eV. In contrast, BHLYP values are much closer to the CCSD(T) ones and the average deviation is only 0.11 eV. Thus, these results indicate that for this particular case BHLYP performs much better than B3LYP. Moreover, the CCSD(T) values obtained for B3LYP geometries are about 0.4 eV higher than those computed for BHLYP geometries. This energy difference mainly arises from the ionized system, which indicates that BHLYP geometries are closer to the ones that one would obtain for the CCSD(T) minima. From the comparison with CCSD(T) results we conclude that the BHLYP is a better choice than B3LYP not only because it yields a localized electron hole, but also because it yields smaller errors for the ionization energy.

The reliability of the results depends on the accuracy of the QM method used and on the convergence of the QM-Pot results to the fully periodic QM limit. To assess the accuracy of BHLYP/6-31++G(d,p):L1 calculations, CCSD(T) calculations with the 6-31++G(d,p) basis set are not sufficient, but merely provide a first guess beyond DFT. Therefore, we have made CCSD(T) calculations with the cc-pVXZ and aug-cc-pVXZ basis sets of Dunning *et al.*, which permit extrapolation to the complete basis set limit.[37] Results are presented in Table V. Enlarging the basis set produces a monotonic increase of the ionization energy. The most accurate nonextrapolated result is 9.91 eV (cc-pVQZ and aug-cc-pVTZ), while cc-pVXZ ($X=T$ and Q) and aug-cc-pVXZ ($X=D$ and T) extrapolations yield 10.02 and 9.97 eV, respectively. Since the BHLYP/6-31++G(d,p) result for the 1T model is 9.47 eV, the CCSD(T) calculations imply an increment of 0.44 to 0.55 eV which should be added to the BHLYP/6-31++G(d,p):L1 results also for larger models.

Besides the high-level (QM) calculation, the accuracy of the total ionization energy also depends on the low-level results for the long-range stabilization of the generated positive charge. This effect is substantial, -0.99 and -1.52 eV for the vertical and adiabatic ionization, respectively (Table III). These values appear to be reasonable since the classical Born model[43] predicts a value of the same order of magnitude (-1.05 eV) for a charge in a spherical cavity of radius 4.7 Å (average distance between link H atoms at the border of the 5T cluster and the generated positive charge). Moreover, previous studies on charged point defects on SiO_2 have estimated similar values for the long-range effects using the Born model[43] or the Isodensity Polarized Continuum Model.[44,12]

TABLE V. Ionization energy (in eV) computed by CCSD(T) for the 1T cluster at the BHLYP:L1 optimized geometry of the 5T cluster.

	X	cc-pVXZ	aug-cc-pVXZ
H-ZSM-5	D	9.16	9.75
	T	9.68	9.91
	Q	9.91	
	Extrap.	10.02	9.97
Silicalite	D		10.72
	T		10.93
	Extrap.		11.00

The reliability of the QM-Pot result for the long-range correction can be tested by increasing the size of the embedded cluster. To this end we have performed single point calculations for the large 25T cluster at the optimized geometry of the embedded 5T cluster. Table VI compares the BHLYP/6-31++G(d,p):L1 results for the 5T and 25T embedded clusters. The total ionization energy (I_A) increases by 0.21 eV yielding 7.95 eV. If the QM-Pot method worked perfectly the same total ionization energy should result for both cluster sizes and, when passing from 5T to 25T, a decrease in the (negative) long-range correction should be accompanied by the same decrease in the (positive) QM contribution. Table VI shows that the reduction of the long-range effect, ΔLR, is larger than the change of the QM contribution, ΔQM. This indicates that the embedding shell-model potential overestimates the long-range effects and the ratio $f=\Delta\mathrm{QM}/\Delta\mathrm{LR}=0.682$ can be used to scale the long-range correction. The improved estimate for the total ionization energy, $I_A=I(\mathrm{QM})+fI(\mathrm{LR})+\mathrm{APC}=8.33$ eV, is 0.59 eV above the 5 T embedded cluster result.

We conclude that an increment of 0.21–0.59 eV should be added to the 5T embedded cluster result ($I=7.74$ eV) to account for the limited size of the embedded cluster and possible errors in the QM-Pot description of long-range effects. This and the increment of 0.44–0.55 eV for the CCSD(T) correction suggest that the 5T embedded cluster

TABLE VI. Vertical (V) and adiabatic (A) ionization energy (in eV) of H-ZSM-5 and silicalite considering embedded clusters of increasing size (L1 interatomic potential parametrization).

	Model		I[a]	QM[b]	LR[c]	$f\times$LR[d]	I-c[e,a]
H-ZSM-5	5T	V	8.94	9.93	−1.33	−0.91	9.36
	5T	A	7.74	9.26	−1.86	−1.27	8.33
	25T//5T[f]	A	7.95	8.81	−1.20	−0.82	8.33
Silicalite	5T	V	9.56	10.61	−1.39	−0.95	10.00
	5T	A	8.31	9.55	−1.58	−1.08	8.82
	25T//5T[f]	A	8.49	9.18	−1.03	−0.70	8.82

[a]Includes aperiodic correction of 0.34 eV.
[b]QM contribution, defined by Eq. (4).
[c]Long-range contribution defined by Eq. (5).
[d]$f=0.682$.
[e]Calculated with corrected long-range contribution $f\times$LR.
[f]Single point calculation at 5T BHLYP:L1 optimized geometry.

result [BHLYP/6-31++G(*d*,*p*):L1] is underestimated by 0.65–1.14 eV. Therefore, our best estimates for the vertical and the adiabatic ionization energies of H-ZSM-5 are 9.6–10.1 eV and 8.4–8.9 eV, respectively.

B. Silicalite

To analyze the effect of Si/Al substitution we have also studied silicalite. We have used BHLYP/6-31++G(*d*,*p*) with the L1 hole parametrization for the 5T embedded cluster. Optimized geometry parameters have been included in Table I. Silicalite shows four Si-O distances in the narrow range of 1.609–1.620 Å. Geometry relaxation due to ionization follows the same trends as in H-ZSM-5; that is, one of the Si-O distances of the central tetrahedron becomes much longer, the elongation being associated with a localized spin distribution over O_1 (Tables I and II). Table VI shows the vertical and adiabatic ionization energies. As for H-ZSM-5 the effect of geometry relaxation on the ionization energy is important, the difference between vertical and adiabatic results is 1.25 eV. Moreover, long range effects show an important stabilization of the positive charge due to the whole framework. The ionization energies of silicalite are about 0.6 eV higher than that of H-ZSM-5.

To refine the obtained energies we have applied the same method and cluster size corrections as for H-ZSM-5. We have analyzed the limitations of BHLYP for these systems performing CCSD(T) calculations on a 1T cluster at the geometry of the optimized 5T BHLYP one. In addition to this, we have also tested the performance of the low-level by enlarging the cluster up to 25T. Results are presented in Tables IV, V, and VI.

For the one-tetrahedron model of silicalite, the BHLYP/6-31++G(*d*,*p*) ionization energy is 0.28 eV lower than that obtained with CCSD(T)/6-31++G(*d*,*p*). This difference is slightly higher that the one observed for H-ZSM-5. Extrapolation to complete basis set using the aug-cc-pV*X*Z (*X*=D and *T*) basis sets increases the ionization energy by 0.68 eV compared to BHLYP/6-31++G(*d*,*p*) (Table V). As for H-ZSM-5, enlarging the cluster lowers the QM contribution, but also decreases (in absolute terms) the stabilizing long-range effects. The total ionization energy increases by 0.18 eV (25T cluster result) to 0.51 eV (after scaling the long-range correction). Applying both increments, for silicalite our best values are 10.4–10.75 eV and 9.2–9.5 eV for vertical and adiabatic processes. The value reported for the valence band edge of SiO_2 is 10.2–10.6 eV,[16] but these results refer to dense silica polymorphs, while silicalite used for the calculations is a microporous material with a much lower density.

The comparison between H-ZSM5 (Si/Al=95) and silicalite reveals that the process is equivalent in both cases and that a localized hole is formed. Moreover, the substitution of aluminum (together with hydrogen) for silicon produces a decrease of the ionization energy of 0.6–0.7 eV as observed in experiments.[17]

TABLE VII. Deprotonation energy (in eV) of neutral and ionized H-ZSM-5.

	ΔE	QM	LR[a]+APC[b]
Neutral	12.86	13.48	−0.62
Ionized	11.40	9.82	1.58

[a]LR contribution defined by Eq. (5).
[b]Aperiodic correction equal to 0.34 eV.

C. Deprotonation

An important property of H^+-exchanged zeolites is their acidity, which affects the adsorption properties and reactivity. For this reason we have studied the deprotonation of the neutral and ionized H-ZSM-5. The deprotonation energy is a measure of acidity strength. Geometry parameters of the $[AlO_4]^{\cdot}$ sites in deprotonated ionized ZSM-5 follow the same trends reported for $[AlO_4H]^{\cdot+}$ and $[SiO_4]^{\cdot+}$ sites in ionized H-ZSM-5 and silicalite (Table I). This is not surprising considering that deprotonation does not affect the spin distribution (Table II). Table VII presents the computed deprotonation energies for the neutral and ionized systems and scheme 1 shows a simple thermodynamic cycle which summarizes the deprotonation energies of HZSM-5 and ionized HZSM-5 as well as the ionization energies of H-ZSM-5 and deprotonated ZSM-5.

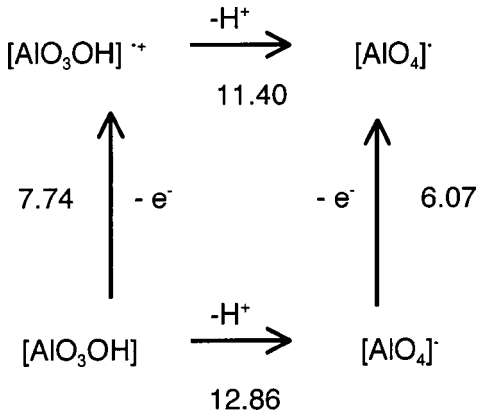

The BHLYP/6-31++G(*d*,*p*) deprotonation energy for the neutral system (12.86 eV) is close to the B3LYP/TZP-DZP result for the 5T embedded cluster model (12.74 eV, all details as in Ref. 21). Previously reported Hartree-Fock values for this site in H-ZSM-5 are 13.28 eV, after correcting for electron correlation effects 12.80 eV.[45]

For the ionized system the calculated deprotonation energy is 11.40 eV. Thus, the generation of a positively charged defect (electron hole) in the zeolite framework decreases the deprotonation energy, i.e., increases the acidity. However, this increase is smaller than the one normally observed for conversion of gas phase molecules into radical cations.[46] Two effects can account for this difference. On the one hand, on ionization of H-ZSM-5 the positive charge is not generated at the oxygen atom that supports the proton. On the other hand, there is a large stabilization of the positive charge due to the whole zeolite framework.

IV. SUMMARY

Formation of an electron hole on an $[AlO_4H]$ center of H-ZSM-5 has been studied for embedded cluster models us-

ing a hybrid QM/ion-pair shell-model potential approach. The two different hybrid density functionals, B3LYP and BHLYP, yield different types of electron holes: delocalized for B3LYP and localized for BHLYP. Inclusion of 50% of exact exchange is enough to obtain localization of the hole. CCSD(T) calculations for the 1T $Al(OH)_4H$ cluster model indicate that the localized description obtained with BHLYP is more accurate, which in agreement with previous findings[13] points to the importance of exact exchange in the functional.

Generation of the electron hole produces substantial geometry relaxation. One Al-O distance, the one to the oxygen with the unpaired electron, increases considerably, while the other three distances slightly decrease. Long-range effects of the zeolite framework stabilize the positively charged electron hole defect.

Our best estimates for the ionization energies of H-ZSM-5 (considering QM method and cluster size corrections) are 9.6–10.1 eV and 8.4–8.9 eV for vertical and adiabatic ionization energies. The substitution of Si for Al,H (change from H-ZSM-5 to silicalite) produces an increase of the ionization energy of about 0.6–0.7 eV, which is in good agreement with ultra-violet photoelectron spectroscopy (UPS) experiments[17] and with the reported valence band edge of SiO_2 (10.2–10.6 eV).[16]

The deprotonation energy of ionized H-ZSM-5 has also been computed. Removing one electron from H-ZSM-5 decreases the deprotonation energy from 12.86 to 11.40 eV. The increase of acidity upon ionization is, however, smaller than that observed for radical cations in the gas phase.

ACKNOWLEDGMENTS

Financial support from MCYT and FEDER (Project No. BQU2002-04112-C02-01), DURSI (Project No. 2001SGR-00182), and the use of the computational facilities of the Catalonia Supercomputer Center (CESCA) are gratefully acknowledged. Financial support for X.S.M.'s stay at Humboldt University from the Generalitat de Catalunya is gratefully appreciated. Thanks go to Christian Tuma for assistance with parallel DFT calculations. This work has been supported by Deutsche Forschungsgemeinschaft within the priority program 1155.

[1] S. E. Sen, S. M. Smith, and K. A. Sullivan, Tetrahedron **55**, 12657 (1999).
[2] A. Dyer, in *Encyclopedia of Inorganic Chemistry* (Wiley, Chichester, 1994), pp. 4363.
[3] H. García, V. Martí, I. Casades, V. Fornés, and H. D. Roth, Phys. Chem. Chem. Phys. **3**, 2955 (2001).
[4] V. Ramamurthy, J. V. Caspar, and D. R. Corbin, J. Am. Chem. Soc. **113**, 594 (1991); K. Pitchumani, D. R. Corbin, and V. Ramamurthy, *ibid.* **118**, 8152 (1996).
[5] P. S. Lakkaraju, K. Shen, H. D. Roth, and H. García, J. Phys. Chem. A **103**, 7381 (1999); H. D. Roth, T. Herbertz, P. S. Lakkaraju, G. Sluggett, and N. J. Turro, *ibid.* **103**, 11350 (1999); M. L. Cano, A. Corma, V. Fornés, and H. García, J. Phys. Chem. **99**, 4241 (1995); M. L. Cano, F. L. Cozens, V. Fornés, H. García, and J. C. Scaiano, *ibid.* **100**, 18145 (1996); X. Liu and J. K. Thomas, Langmuir **9**, 727 (1993); M. Bonora, M. Brustolon, L. Storaro, M. Casagrande, D. Biglino, Y. Itagaki, U. Segre, and M. Lenarda, Phys. Chem. Chem. Phys. **2**, 4823 (2000).
[6] E. A. Piocos, P. Han, and D. W. Werst, J. Phys. Chem. **100**, 7191 (1996); M. V. Barnabas, D. W. Werst, and A. D. Trifunac, Chem. Phys. Lett. **206**, 21 (1993); K. R. Cromack, D. W. Werst, M. V. Barnabas, and A. D. Trifunac, *ibid.* **218**, 485 (1994); R. Erickson, N. P. Benetis, A. Lund, and M. Lindgren, J. Phys. Chem. A **101**, 2390 (1997); D. W. Werst, E. A. Piocos, E. E. Tartakovsky, and A. D. Trifunac, Chem. Phys. Lett. **229**, 421 (1994); D. W. Werst, E. E. Tartakovsky, E. A. Piocos, and A. D. Trifunac, J. Phys. Chem. B **98**, 10249 (1994); F. L. Cozens, R. Bogdanova, M. Régimbald, H. García, V. Martí, and J. C. Scaiano, *ibid.* **101**, 6921 (1997).
[7] E. A. Piocos, D. W. Werst, A. D. Trifunac, and L. A. Eriksson, J. Phys. Chem. **100**, 8408 (1996); D. W. Werst, P. Han, S. C. Choure, E. I. Vinokur, L. Xu, A. D. Trifunac, and L. A. Eriksson, J. Phys. Chem. B **103**, 9219 (1999).
[8] H. García and H. D. Roth, Chem. Rev. (Washington, D.C.) **102**, 3947 (2002).
[9] X. Zhang, C. K. Ong, and A. M. Stoneham, J. Phys.: Condens. Matter **6**, 5647 (1994).
[10] M. Boero, A. Pasquarello, J. Sarnthein, and R. Car, Phys. Rev. Lett. **78**, 887 (1997); G. Pacchioni and A. Basile, Phys. Rev. B **60**, 9990 (1999); A. H. Edwards, Phys. Rev. Lett. **71**, 3190 (1993).
[11] D. L. Griscom, Phys. Rev. B **40**, 4224 (1989); D. L. Griscom, J. Non-Cryst. Solids **149**, 137 (1992).
[12] D. Erbetta, D. Ricci, and G. Pacchioni, J. Chem. Phys. **113**, 10744 (2000).
[13] G. Pacchioni, F. Frigoli, D. Ricci, and J. A. Weil, Phys. Rev. B **63**, 054102 (2001); J. Lægsgaard and K. Stokbro, Phys. Rev. Lett. **86**, 2834 (2001).
[14] R. H. D. Nuttall and J. A. Weil, Can. J. Phys. **59**, 1696 (1981); M. J. Mombourquette, J. A. Weil, and P. G. Mezey, *ibid.* **62**, 21 (1984).
[15] M. Sodupe, J. Bertran, L. Rodríguez-Santiago, and E. J. Baerends, J. Phys. Chem. A **103**, 166 (1999); M. Grüning, O. V. Gritsenko, S. J. A. van Gisbergen, and E. J. Baerends, *ibid.* **105**, 9211 (2001); J. Oxgaard and O. Wiest, *ibid.* **105**, 8236 (2001); B. Braïda, P. C. Hiberty, and A. Savin, *ibid.* **102**, 7872 (1998).
[16] H. Ibach and J. E. Rowe, Phys. Rev. B **10**, 710 (1974); D. L. Griscom, J. Non-Cryst. Solids **24**, 155 (1977).
[17] T. L. Barr, Zeolites **10**, 760 (1990); T. L. Barr, L. M. Chen, M. Mohsenian, and M. A. Lishka, J. Am. Chem. Soc. **110**, 7962 (1988); B. Herreros, H. He, T. L. Barr, and J. Klinowski, J. Phys. Chem. **98**, 1302 (1994); W. Grünert, M. Muhler, and H. G. Karge, J. Chem. Soc., Faraday Trans. **92**, 701 (1996).
[18] M. Sierka and J. Sauer, J. Chem. Phys. **112**, 6983 (2000).
[19] U. Eichler, C. M. Kölmel, and J. Sauer, J. Comput. Chem. **18**, 463 (1997).
[20] L. Rodríguez-Santiago, M. Sierka, V. Branchadell, M. Sodupe, and J. Sauer, J. Am. Chem. Soc. **120**, 1545 (1998); L. A. Clark, M. Sierka, and J. Sauer, *ibid.* **125**, 2136 (2003).
[21] M. Sierka and J. Sauer, J. Phys. Chem. B **105**, 1603 (2001).
[22] D. Nachtigallová, P. Nachtigall, M. Sierka, and J. Sauer, Phys. Chem. Chem. Phys. **1**, 2019 (1999).
[23] R. Ahlrichs, M. Bär, M. Häser, H. Horn, and C. Kölmel, Chem. Phys. Lett. **162**, 165 (1989); O. Treutler and R. Ahlrichs, J. Chem. Phys. **102**, 346 (1995).
[24] J. D. Gale, J. Chem. Soc., Faraday Trans. **93**, 629 (1997).
[25] H. Van Koningsveld, J. C. Jansen, and H. van Bekkum, Zeolites **10**, 235 (1990).
[26] K.-P. Schröder, J. Sauer, M. Leslie, and C. R. A. Catlow, Zeolites **12**, 20 (1992).
[27] A. D. Becke, J. Chem. Phys. **98**, 5648 (1993).
[28] C. Lee, W. Yang, and R. G. Parr, Phys. Rev. B **37**, 785 (1988).
[29] A. D. Becke, J. Chem. Phys. **98**, 1372 (1993).
[30] R. Ditchfield, W. J. Hehre, and J. A. Pople, J. Chem. Phys. **54**, 724 (1971); W. J. Hehre, R. Ditchfield, and J. A. Pople, *ibid.* **56**, 2257 (1972).
[31] K. Raghavachari, G. W. Trucks, J. A. Pople, and M. Head-Gordon, Chem. Phys. Lett. **157**, 479 (1989).
[32] P. J. Knowles, C. Hampel, and H.-J. Werner, J. Chem. Phys. **99**, 5219 (1993).
[33] MOLPRO is a package of *ab initio* programs written by H. J. Werner and P. J. Knowles, with contributions from R. D. Amos, A. Bernhardsson, A. Berning *et al.*,
[34] C. Hampel, K. Peterson, and H.-J. Werner, Chem. Phys. Lett. **190**, 1 (1992), and references therein. The program to compute the perturbative triples corrections has been developed by M. J. O. Deegan and P. J. Knowles.
[35] T. H. Dunning, J. Chem. Phys. **90**, 1007 (1989).
[36] R. A. Kendall, T. H. Dunning, and R. J. Harrison, J. Chem. Phys. **96**, 6796 (1992).
[37] A. Halkier, T. Helgaker, P. Jørgensen, W. Klopper, H. Koch, J. Olsen, and A. K. Wilson, Chem. Phys. Lett. **286**, 243 (1998).

[38] C. R. A. Catlow, M. Dixon, and W. C. Mackrodt, in *Computer Simulations of Solids*, edited by C. R. A. Catlow and W. C. Mackrodt (Springer, Berlin, 1982), Vol. 166.
[39] M. Sierka and J. Sauer, Faraday Discuss. **106**, 41 (1997).
[40] X. Zhang and C. K. Ong, J. Phys.: Condens. Matter **7**, 8577 (1995); F. Sim, C. R. A. Catlow, M. Dupuis, and J. D. Watts, J. Chem. Phys. **95**, 4215 (1991).
[41] M. Leslie and M. J. Gillan, Solid State Phys. **18**, 973 (1985); U. Eichler, M. Brändle, and J. Sauer, J. Phys. Chem. B **101**, 10035 (1997).
[42] C. Ehrhardt and R. Ahlrichs, Theor. Chim. Acta **68**, 231 (1985).
[43] M. Born, Z. Phys. **45**, 1 (1920).
[44] J. B. Foresman, T. A. Keith, K. B. Wiberg, J. Snoonian, and M. J. Frisch, J. Phys. Chem. **100**, 16098 (1996).
[45] M. Brändle and J. Sauer, J. Am. Chem. Soc. **120**, 1556 (1998).
[46] A. Gil, J. Bertran, and M. Sodupe, J. Am. Chem. Soc. **125**, 7461 (2003); F. G. Bordwell and J.-P. Cheng, *ibid.* **111**, 1792 (1989).